Structural Characterization of Adenine Nucleotides Bound to *Escherichia coli* Adenylate Kinase. 2. ^{31}P and ^{13}C Relaxation Measurements in the Presence of Cobalt(II) and Manganese(II)†

Yan Lin‡ and B. D. Nageswara Rao*

Department of Physics, Indiana University Purdue University Indianapolis, 402 North Blackford Street, Indianapolis, Indiana 46202-3273

Received October 22, 1999; Revised Manuscript Received December 22, 1999

ABSTRACT: ^{13}C spin−lattice relaxation rates have been measured for two complexes of *Escherichia coli* adenylate kinase (AKe), viz., AKe•[U-^{13}C]ATP and AKe•[U-^{13}C]AMP•GDP in the presence of the substituent activating paramagnetic cation Mn(II) for the purpose of determination of the enzyme-bound conformations of ATP and AMP. (GDP has been added to the AMP complex with the enzyme in order to hold the cation in the bound complex.) Measurements of relaxation times at three different ^{13}C frequencies, 181.0, 125.7, and 75.4 MHz, indicate that the relaxation times in the enzyme−nucleotide complexes with the paramagnetic cation are not exchange-limited; i.e., they are larger than the effective lifetimes of cation binding to these complexes and are, therefore, dependent on the cation−^{13}C distances. An analysis of the frequency-dependent relaxation data allowed all of the ten Mn(II)−^{13}C distances to be determined in each of the complexes. Similar measurements of the ^{31}P relaxation rate made on AKe•ATP and AKe•AMP•GDP complexes in the presence of Co(II) as the activating cation yielded Co(II)−^{31}P distances for each adenine nucleotide. These distances, together with the interproton distances determined previously from TRNOESY experiments [Lin, Y., and Nageswara Rao, B. D. (2000) *Biochemistry 39*, 3636−3646], led to a complete characterization of both ATP and AMP conformations in AKe-bound complexes. These conformations differ significantly from the nucleotide conformations in crystals of AKe•AP_5A and AKe•AMP•AMPPNP as determined by X-ray crystallography.

This paper presents structure measurements aimed at a complete structural characterization of AMP[1] and ATP bound to *Escherichia coli.* adenylate kinase (AKe), which catalyzes the reaction

$$\text{AMP} + \text{M(II)ATP} \leftrightarrow \text{ADP} + \text{M(II)ADP}$$

where M(II) is an obligatory divalent cation. In vivo, M(II) is Mg(II), and in vitro, activating paramagnetic cations Mn(II) and Co(II) may be substituted. Nucleotides, free in solution, possess considerable internal mobility and are likely to assume a unique conformation appropriate for catalysis when they are enzyme-bound (*1*). Therefore, a complete structural characterization of these bound nucleotides requires the specification of a number of distances between different nuclei in the molecule, as well as those with reference to a well-defined external point. In the accompanying paper (*2*), results of TRNOESY experiments yielding interproton distances that allow a determination of the glycosidic torsion angle, and sugar pucker, characterizing the adenosine conformations of AMP and MgATP bound to the enzyme, have been presented. In the present paper, distance determinations with respect to the substituent activating paramagnetic cations, Mn(II) and Co(II), made on the basis of distance-dependent enhancements of spin relaxation rates of nuclei in the vicinity of the cations are presented. The distance data obtained by both of these approaches allow a complete characterization of the conformations of both AMP and ATP bound to adenylate kinase.

Four groups of measurements of paramagnetic enhancement of spin relaxation have been made: ^{13}C relaxation measurements on AKe•[U-^{13}C]ATP and AKe•[U-^{13}C]AMP•GDP complexes with Mn(II) and ^{31}P relaxation measurements on AKe•ATP and AKe•AMP•GDP complexes with Co(II). ^{31}P relaxation measurements of this kind on the Co(II) complexes, previously published for porcine muscle adenylate kinase (AKp) over a decade ago (*3*), established the chelation pattern of the cation with the phosphate chain. The experiments had to be performed with Co(II), since the ^{31}P relaxation times in the Mn(II) complexes were much shorter than the effective lifetimes of the cation in these complexes, and hence bereft of structural information about

† Supported in part by the National Institutes of Health (GM43966) and IUPUI. This work forms part of a thesis for which Y.L. was awarded a Ph.D. degree in physics by Purdue University in 1999. Part of these results were presented at the 39th Experimental NMR Conference (ENC) held at Asilomar, CA, March 22−27, 1998.

* To whom correspondence should be addressed. Phone: (317) 274-6897. Fax: (317) 274-2393. E-mail: brao@iupui.edu.

‡ Present address: Department of Biochemistry & Biophysics, School of Medicine, University of Pennsylvania, Philadelphia, PA 19104-6059.

[1] Abbreviations: 2D, two dimensional; ADP, adenosine 5′-diphosphate; AK, adenylate kinase; AKe, *Escherichia coli* adenylate kinase; AKp, porcine muscle adenylate kinase; AMP, adenosine 5′-monophosphate; AMPPNP, adenylylimidodiphosphate; AP_5A, P^1,P^5-bis(5′-adenosyl)pentaphosphate; ATP, adenosine 5′-triphosphate; U-^{13}C, uniformly labeled with ^{13}C; GDP, guanosine 5′-diphosphate; Hepes, *N*-(2-hydroxyethyl)piperazine-*N*′-2-ethanesulfonic acid; NMR, nuclear magnetic resonance; PDB, Protein Data Bank; SAX, strong anion exchange; SPE, solid-phase extraction; TRNOESY, transferred two-dimensional nuclear Overhauser effect spectroscopy.

10.1021/bi992460e CCC: $19.00
Published on Web 03/07/2000

ATP. The measurements with Co(II) are repeated here to verify if the cation is similarly chelated to ATP bound to AKe. It should be noted that the purpose of including GDP in the AMP complexes is to hold the cation at the active site so that distances could be determined with respect to it on the basis of spin relaxation rate enhancements of substrate nuclei. GTP could not be used for this purpose because adenylate kinase also catalyzes the reaction

$$\text{AMP} + \text{M(II)GTP} \leftrightarrow \text{ADP} + \text{M(II)GDP}$$

The main thrust of the experiments reported here pertains to ^{13}C spin relaxation measurements in Mn(II) complexes with [U-^{13}C]nucleotides bound to the enzyme, leading to the determination of the distances of all 10 ^{13}C nuclei in adenosine with respect to the cation, which is chelated to the phosphate chain of the nucleotide at the ATP site on the enzyme. With adenosine conformations of the nucleotides already determined by TRNOESY measurements (*2*), these 10 ^{13}C distances with respect to the cation represent the final set of distances needed for a complete characterization of the nucleotide conformation. The first example of ^{13}C relaxation measurements of this kind was reported recently by Raghunathan et al. (*4*) for nucleotide complexes of 3-phosphoglycerate kinase.

The motivation and rationale behind the NMR determination of enzyme-bound substrate conformation in solution phase arise in part from some inadequacies in the crystallographic data, among which is the failure to locate the cation at the active site. Since the distance data from relaxation enhancement are determined with respect to the cation, the location of the cation at the active site is unequivocal in the structures obtained on the basis of the NMR measurements.

EXPERIMENTAL PROCEDURES

Materials. AMP, ATP, AMPPNP, 0.1 mM $MnCl_2$ solution in 0.15 M NaCl, glucose, and hexokinase were purchased from Sigma Chemical Co., Puratronic $CoCl_2 \cdot 6H_2O$ was from Alfa Aesar, DEAE-cellulose was from Whatman, Blue-Sepharose resin was from Pharmacia, 99.9% D_2O was from Cambridge Isotope Laboratories, Hepes was from Research Organics Inc., [U-^{13}C]ATP was from Isotech, GDP from Boehringer Mannheim, Chelex-100 was from Bio-Rad Laboratories, and SAX and C18 solid-phase extraction cartridges were from Varian Sample Preparation Products. All other chemicals used were of analytical reagent grade.

Sample Preparation. An expression system of AKe was kindly provided by Professor Paul Rösch, Universität of Bayreuth, Bayreuth, Germany. The purification of the enzyme was performed following published procedures (*5*). The purity of the enzyme was ascertained by electrophoresis, and the specific activity of the enzyme, assayed by monitoring the formation of ADP by coupling with pyruvate kinase and lactate dehydrogenase reactions (*6*), is usually $\sim$ 800 units/mg.

For the NMR experiments the purified enzyme was dialyzed against 50 mM Hepes-K^+, pH 8.0, containing preequilibrated Chelex-100 resin to eliminate trace amounts of metal ion contamination from the sample. The enzyme was then concentrated to $\sim$50 mg/mL in an Amicon ultrafiltration concentrator, lyophilized, and redissolved in chelexed D_2O to one-fourth of the volume used before lyophilization so that the buffer concentration increased to $\sim$200 mM and the protein concentration to $\sim$200 mg/mL. The pH of nucleotide solutions was adjusted to 8.0 before the solutions were passed through a Chelex-100 column. They were then lyophilized and stored at -20 °C. The final dissolution of the nucleotides in D_2O was made immediately before addition to the enzyme. The concentrations of the nucleotides and of the enzyme were determined spectrophotometrically with extinction coefficients $\epsilon_{259}^{mM} = 15.4$ cm^{-1} for AMP, ATP, and AMPPNP, $\epsilon_{252}^{mM} = 13.7$ cm^{-1} for GDP, and $\epsilon_{280}^{mg/mL} = 0.5$ cm^{-1} for the enzyme (molecular mass 23.6 kDa) (*7*). The pH values reported are direct pH meter readings for the prepared samples, uncorrected for the presence of D_2O. All buffer solutions were passed through a Chelex-100 column to remove trace metal impurities.

[U-^{13}C]ATP was purchased from Isotec. However, this nucleotide required further purification by solid-phase extraction using SAX cartridges. With a stepwise salt gradient of 10$-$200 mM ammonium bicarbonate, pH 8.0, AMP elutes first and ATP last. Fractions were checked by NMR as well as by optical absorption at 259 nm. Separated adenine nucleotides were processed individually by repeated rotovaporation with 5$-$10 additions of 2 mL portions of methanol to decompose the ammonium bicarbonate, followed by passage through a Chelex-100 (Bio-Rad) column to remove metal ion contamination. The purity was then checked by ^{31}P NMR.

[U-^{13}C]AMP was synthesized from [U-^{13}C]ATP by coupled reactions of adenylate kinase and hexokinase and was further isolated from the reaction mixture on a C18 SPE column with a methanol/H_2O (v:v = 4:1) elution.

NMR Measurements. ^{31}P NMR measurements on AKe·Co(II)ATP and AKe·AMP·Co(II)GDP at 202 MHz were made on a Varian UNITY 500 spectrometer, ^{13}C NMR measurements on AKe·MnATP and AKe·AMP·MnGDP at 75 and 125 MHz on Varian UNITY 300 and INOVA 500 spectrometers at the NMR Center of IUPUI, and those at 181 MHz were made on a UNITY-Plus 720 spectrometer at the National High Magnetic Field Laboratory, Tallahassee, FL. All the spectrometers are equipped with 10-mm broad-band probes and high-stability variable-temperature controllers. Measurements were made at 5 °C. NMR sample volumes were 2 mL, contained in a 10-mm o.d. NMR tube. D_2O was added directly to the sample for field-frequency lock. Typical sample contents were 3.5$-$5.7 mM AKe and 2.0$-$4.1 mM nucleotides, with cation concentrations varied between 0 and 5% of the ATP concentration in the AKe·ATP complex experiments and between 0 and 10% of the AMP concentration in the AKe·AMP·GDP complex experiments (see footnotes of Tables 1 and 2 for further details). The relative concentrations of the enzyme and nucleotide were chosen on the basis of known dissociation constants (*8*), such that free nucleotide concentrations were kept at $<$3% in all experiments.

T_1 measurements were made using the standard inversion recovery sequence with a composite π pulse (*9*). Frequency-modulated broad-band decoupling was used to obtain proton-decoupled ^{13}C NMR spectra. ^{31}P NMR was frequently used to check the condition of these NMR samples, and no significant ATP hydrolysis was found at the end of all the measurements.

Molecular Modeling. Molecular dynamics (MD) simulations and energy minimizations were carried out on a Silicon Graphics Octane computer, running IRIX 6.4, using the program SYBYL 6.5 from Tripos Inc., St. Louis, MO. The Tripos force field was used for all energy calculations, and the conjugate gradient algorithm was chosen for the minimization. The simulations and calculations were performed on ATP, AMP, and AMPPNP molecules in a vacuum.

Theoretical Details. A detailed description of the theoretical basis and experimental strategy used in the measurement of nuclear spin-relaxation rates in the presence of paramagnetic cations has been presented previously (*10*−*16*). An extension of this theory, useful for analyzing frequency-dependent relaxation rates for multiple nuclei in the same complex, such as the current measurements on enzyme-bound [U-^{13}C]nucleotides, has been given in a recent paper on a similar study of the nucleotide complexes of 3-phosphoglycerate kinase (*4*). Summarized below, in a skeletal form, are the equations relevant to understand the analysis of data presented here.

For a sample containing exchanging paramagnetic (E·M·S) and diamagnetic (E·S) complexes in fractional concentrations of p ($\ll$1) and $(1 - p)$, respectively, the paramagnetic contribution, $(T_{1P})^{-1}$ [observed relaxation rate $(T_{1,obs})^{-1}$ minus the relaxation rate in E·S, $(T_{1D})^{-1}$] is given by

$$(T_{1P})^{-1} = (T_{1,obs})^{-1} - (T_{1D})^{-1} = p/(T_{1M} + \tau_M) \quad (1)$$

where τ_M is the lifetime of the paramagnetic complex and $(T_{1M})^{-1}$ [$\gg(T_{1D})^{-1}$] is the relaxation rate in E·M·S, which is related to the cation−nucleus distance r(Mn−^{13}C) by the relation

$$(T_{1M})^{-1} = (C/r)^6 f(\tau_C) \quad (2)$$

where

$$C = [(2/15)S(S+1)g^2\gamma_I^2\beta^2]^{1/6} \quad (3)$$

$$f(\tau_C) = 3\tau_C/(1 + \omega_I^2\,\tau_C^2) \quad (4)$$

$$\tau_C^{-1} = \tau_R^{-1} + \tau_{S1}^{-1} \quad (5)$$

and

$$\tau_{S1}^{-1} = B[\tau_V/(1 + \omega_S^2\,\tau_V^2) + 4\tau_V/(1 + 4\omega_S^2\,\tau_V^2)] \quad (6)$$

where S, ω_S, and g represent the spin, the EPR frequency, and the isotropic g-factor of the cation in E·M·S, γ_I and ω_I are the gyromagnetic ratio and Larmor frequency of the nucleus, β is the Bohr magneton, τ_C is the correlation time modulating the Mn(II)−^{13}C dipolar interactions (for which C = 512 Å s$^{-1/3}$), τ_R is the isotropic rotational correlation time of the E·M·S complex, τ_{S1} is the longitudinal relaxation time of Mn(II) in E·M·S, B is a constant proportional to the square of the fluctuations in the strength of the crystal field interaction implicit in the chelation of the cation, and τ_V is the correlation time characterizing such fluctuations.

Equations 2−4 show that

$$pT_{1P} - \tau_M = T_{1M} = \left(\frac{r}{C}\right)^6 \frac{1}{f(\tau_C)} = \left(\frac{r}{C}\right)^6 \left[\frac{1}{3\tau_C} + \omega_I^2\left(\frac{\tau_C}{3}\right)\right] \quad (7)$$

If $\omega_S\tau_V \ll 1$, eq 6 gives

$$\tau_{S1}^{-1} = 5B\tau_V \quad (8)$$

τ_C (given by eq 5) becomes frequency independent, and a plot of pT_{1P} vs ω_I^2 will be linear with a slope of $(r/C)^6(\tau_C/3)$ and an intercept given by $[\tau_M + (r/C)^6(1/3\tau_C)]$. On the other hand, if $\omega_S\tau_V \gg 1$, eq 6 reduces to

$$\tau_{S1} = \frac{\tau_V}{2B}\left(\frac{g\beta}{\gamma_I}\right)^2 \omega_I^2 = A\omega_I^2 \quad (9)$$

τ_{S1} and τ_C are now frequency dependent. A plot of pT_{1P} vs ω_I^2 will then be nonlinear.

The analysis of relaxation rates simultaneously measured for multiple nuclei in a complex is simplified by noting that a plot of $(pT_{1P})_1$ values obtained for all the nuclei at $\omega_I = \omega_1$ versus the $(pT_{1P})_2$ values obtained at $\omega_I = \omega_2$ is a straight line, independent of r, as given by

$$\frac{(pT_{1P})_1 - \tau_M}{(pT_{1P})_2 - \tau_M} = \frac{(T_{1M})_1}{(T_{1M})_2} = [(1 + \omega_1^2\,\tau_{C1}^2)/(1 + \omega_2^2\,\tau_{C2}^2)](\tau_{C2}/\tau_{C1}) \quad (10)$$

where τ_{C1} and τ_{C2} are the values of τ_C, and $(T_{1M})_1$ and $(T_{1M})_2$ are the values of T_{1M}, at the two frequencies ω_1 and ω_2, respectively. If pT_{1P} vs ω_I^2 is linear (τ_C is independent of frequency, $\tau_{C1} = \tau_{C2} = \tau_C$), then the slope, R, of the linear plot of $(pT_{1P})_1$ vs $(pT_{1P})_2$ is given by

$$R(\omega_1,\omega_2) = \frac{1 + \omega_1^2\,\tau_C^2}{1 + \omega_2^2\,\tau_C^2} \quad (11)$$

and it may be seen that

$$\tau_C = [(1 - R)/(R\omega_2^2 - \omega_1^2)]^{1/2} \quad (12)$$

and

$$\tau_M = \text{intercept}/(1 - R) \quad (13)$$

On the other hand, if pT_{1P} vs ω_I^2 is nonlinear (τ_C is frequency dependent), eqs 11 and 12 are not applicable. In this case, the values of B and τ_V (and, therefore, the value of τ_{S1} as a function of frequency) can be obtained by fitting the slopes and intercepts for different values of $\omega_1$and ω_2 to eqs 9, 10, and 13 with the help of a computer program.

RESULTS AND ANALYSIS

(A) Location of the Cation with Respect to the Phosphate Chain of ATP: ^{31}P Relaxation Measurements. As mentioned earlier, ^{31}P relaxation measurements of E·ATP complexes in the presence of Co(II) have been made for porcine adenylate kinase (*3*). The results show that the relaxation times are exchange limited ($T_{1M} < \tau_M$) with Mn(II) as the cation and are distance dependent with Co(II). The Co(II)−^{31}P distances calculated are about 3 Å for β-P and γ-P of ATP, showing that Co(II) is directly chelated to these

Table 1: Comparison of Paramagnetic Relaxation Enhancements $p(T_{1P})^{-1}$ (s^{-1}) of ^{31}P Relaxation Rates, Activation Energies ΔE (kcal/mol), and Co(II)−^{31}P Distances r (Å) for AK·M(II)ATP and AK·AMP·M(II)GDP Complexes in the Presence of Mn(II) and Co(II) for Porcine (AKp) and *E. coli* (AKe) Adenylate Kinase

	$p(T_{1P})^{-1}$ s^{-1} (ΔE, kcal/mol)				r (Å)			
	ATP				ATP			
	α-P	β-P	γ-P	AMP	α-P	β-P	γ-P	AMP
AKp·MnATP[a]	660 (6.4)	860 (7.8)	1030 (8.4)					
AKp·CoATP[a]	27 (2.0)	160 (2.0)	230 (2.2)		3.9−5.1	2.9−3.8	2.7−3.6	
AKp·AMP·CoGDP[a]				5.1 (2.0)				5.1−6.8
AKe·MnATP[b]	671 (4.1)	990 (7.0)	1349 (5.6)					
AKe·CoATP[c]	44	243	278		3.6−4.7	2.7−3.5	2.6−3.5	
AKe·AMP·CoGDP[c]				3.8				5.4−7.1

[a] Data taken from Ray et al. (*3*). The measurements were made at 121.4 MHz. Activation energies ΔE (in parentheses) have been determined by measuring T_{1P} as a function of temperature in the range 5−30 °C. [b] Data taken from Ms. X. Lu's M. S. thesis, Department of Physics, IUPUI (1990). The measurements were made at 121.4 MHz. [c] These are present data obtained at 202 MHz. Sample composition: enzyme, 3.2−4.0 mM; nucleotide of interest, 2.0−2.4 mM; $CoCl_2$, 0.024−0.12 and 0.03−0.50 mM for ATP and AMP complexes, respectively. The GDP concentration in the AMP complexes was 2.0 mM.

Table 2: Paramagnetic Effect $p(T_{1P})^{-1}$ (s^{-1}) of Mn(II) on ^{13}C Relaxation Rates at 75, 125, and 181 MHz for AKe·Mn[U-^{13}C]ATP and AKe·[U-^{13}C]AMP·MnGDP Complexes[a]

	AKe·Mn[U-^{13}C]ATP $p(T_{1P})^{-1}$ (s^{-1})			AKe·[U-^{13}C]AMP·MnGDP $p(T_{1P})^{-1}$ (s^{-1})		
nucleus	181 MHz	125 MHz	75 MHz	181 MHz	125 MHz	75 MHz
C2	8.9	10.9	23.2	4.7	n/m[b]	n/m[b]
C4	34.8	51.6	85.5	9.6	29.1	49.5
C5	82.7	103.1	174.1	19.5	70.9	106.0
C6	37.3	49.0	86.0	11.3	39.4	64.8
C8	150.2	249.1	306.7	41.9	143.8	251.2
C1′	26.5	34.2	39.5	3.1	10.9	27.1
C2′	36.2	83.2	126.8	n/m[b]	n/m[b]	44.6
C3′	31.9	60.6	85.2	1.5	7.2	27.2
C4′	46.0	74.8	157.1	3.4	11.7	23.1
C5′	100.3	190.5	244.0	10.9	34.4	44.1

[a] Typical sample concentrations in the experiments were enzyme, 3.8−5.7 mM, and [U-^{13}C]nucleotide, 3.2−4.1 mM. $MnCl_2$ varied between 0 and 0.18, and 0−0.4 mM for ATP and AMP complexes, respectively. GDP concentrations in the AMP complexes were 2.7−4.0 mM. [b] Could not be measured with sufficient accuracy. The data for C2 and C2′ in the AKe·[U-^{13}C]AMP·MnGDP complex, both of which were obtained at a single frequency, were not used to determine τ_M and τ_C appropriate for all the nuclei.

phosphates, but the Co(II)−α-P distance is ∼1.0 Å longer. In the present work, ^{31}P relaxation rates and their activation energies have been measured for AKe·ATP complexes at 202 MHz in the presence of Co(II), and at 121.4 MHz as a function of temperature in the range 5−30 °C in the presence of Mn(II), to determine if the data parallel those for the porcine enzyme. The results are presented in Table 1, along with those previously published for the porcine enzyme. It is evident that the data for the two enzymes are very similar. Note that activation energies of T_{1M} are usually 1−3 kcal/mol, whereas those for τ_M are 5−20 kcal/mol. Furthermore, T_{1M} depends on frequency and τ_M does not. Relaxation times with Mn(II) are exchange limited and those with Co(II) are not. Co(II)−^{31}P distances indicate direct chelation with β-P and γ-P in E·ATP and a longer distance for α-P.

Note that the Co(II)−^{31}P distances in Table 1 have been calculated as ranges using 10^{-12} s < $f(\tau_C)$ < 5×10^{-12} s in eq 2 in view of the lack of a precise theory applicable for relaxation enhancement with Co(II)[2] (*3*, *13*). Nevertheless, the theoretical details outlined above are appropriate for Mn(II) complexes when the relaxation times are not exchange limited ($T_{1M} > \tau_M$), which is the case for ^{13}C nuclei in enzyme complexes of [U-^{13}C]nucleotides located at distances larger than ∼5 Å from Mn(II), as shown below.

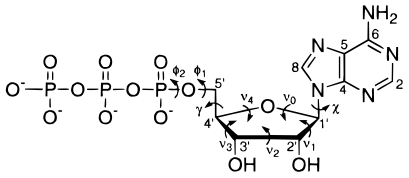

FIGURE 1: Chemical structure of an ATP molecule with carbon numbering and various torsion angles labeled.

(B) Orientation of the Phosphate Chain with Respect to Adenosine: ^{13}C Relaxation Measurements. Figure 1 shows a diagram of the ATP molecule with the various carbons numbered and dihedral angles marked. ^{13}C relaxation rates in AKe·[U-^{13}C]ATP and AKe·[U-^{13}C]AMP·GDP were measured as functions of added Mn(II) concentration to determine $p(T_{1P})^{-1}$. A typical T_1-stack plot for AKe·[U-^{13}C]ATP at 125.7 MHz is shown in Figure 2, along with a juxtaposed proton-decoupled ^{13}C spectrum of [U-^{13}C]ATP free in solution. The identifications of the individual ^{13}C resonances are based on a previously published assignment (*18*). It may be seen that the ^{13}C resonances show negligible (<1 ppm) changes in chemical shifts with respect to those for the free [U-^{13}C]ATP. $^{13}C-^{13}C$ spin couplings between adjacent ^{13}C nuclei, with values of ∼40 Hz for ribose carbons and ∼50−70 Hz for adenine base carbons, are resolved in the spectrum of free [U-^{13}C]ATP. However, in the enzyme-bound complex, the resonances are too broad for the spin−spin splitting to be resolved. The signals for C6 and C2 of the adenine and those for C1′ and C4′ of the ribose overlap, and in these cases deconvolution procedures have been used to delineate the T_1 values.

The ^{13}C relaxation rates $p(T_{1P})^{-1}$ measured at three different frequencies, 181.0, 125.7, and 75.4 MHz, are given in Table 2 for both AKe·Mn[U-^{13}C]ATP and AKe·[U-^{13}C]-

[2] The uncertainty in $f(\tau_C)$ is related to the fact that the applicability of the conventional theory of electron relaxation, which leads to eq 6, for example, is questionable for Co(II) complexes. Furthermore, there is also some ambiguity in the constant C (eq 2) due to g-tensor anisotropy of Co(II) (*11*−*13*, *17*). However, since C and $f(\tau_C)$ occur as a product $C^6 f(\tau_C)$ in eq 2, the range of a factor of 5 chosen for the uncertainty in $f(\tau_C)$ (as stated) implicitly covers the uncertainty in both of these parameters.

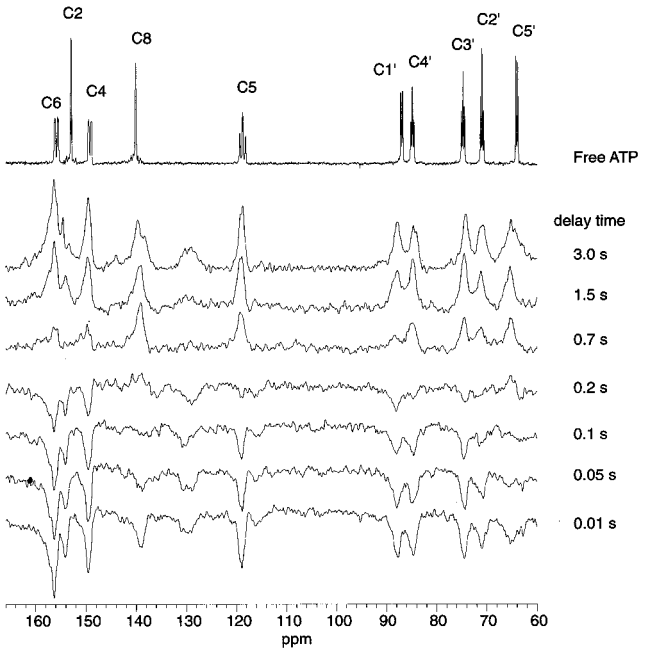

FIGURE 2: Typical stack plot of proton-decoupled ^{13}C T_1 measurements of the AKe·Mn[U-^{13}C]ATP complex at 125.7 MHz and 5 °C. The proton-decoupled ^{13}C spectrum of free [U-^{13}C]ATP is juxtaposed with ^{13}C assignments labeled. Delay times after the inversion are given in the spectra. The sample contained 4.2 mM AKe, 3.5 mM [U-^{13}C]ATP, and 0.08 mM $MnCl_2$. See Figure 1 for carbon numbering.

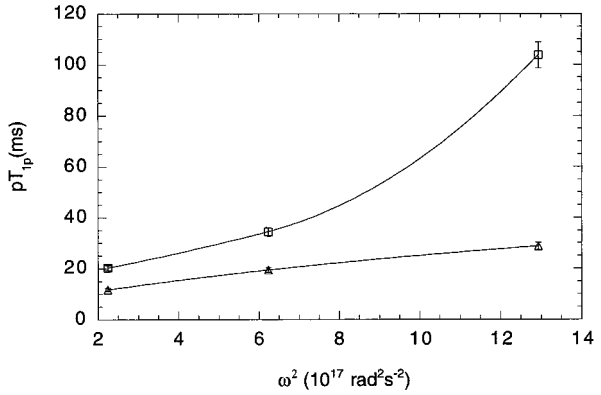

FIGURE 3: Frequency dependence of the observed relaxation rate shown as plots of pT_{1P} vs ω_I^2 (square of ^{13}C frequency) for C4 in AKe·Mn[U-^{13}C]ATP (△) and AKe·[U-^{13}C]AMP·MnGDP (□) complexes. Solid lines are drawn through theoretically calculated data points for each complex. The parameters used in the calculations are $r = 9.2$ Å and $B\tau_V = 1.37 \times 10^8$ s^{-1} for the ATP complex and $r = 9.5$ Å and $\tau_V/B = 2.1 \times 10^{-33}$ s^{-3} for the AMP complex.

AMP·MnGDP complexes. Plots of pT_{1P} vs ω_I^2 for the C4 carbon in the two complexes, shown in Figure 3, indicate that the frequency dependence of the relaxation is qualitatively different in these two complexes. The plot for E·MnATP is linear whereas there is appreciable curvature in that for E·AMP·MnGDP. The data for each of the ^{13}C nuclei in the two complexes display similar contrasting frequency dependence. The linear dependence of pT_{1P} vs ω_I^2 for the E·Mn[U-^{13}C]ATP complex suggests that τ_C is independent of frequency, whereas the nonlinearity in the plot for the E·[U-^{13}C]AMP·MnGDP complex indicates that τ_{S1} is frequency dependent.

Further analysis of the data was performed on the basis of slopes and intercepts of p$T_{1P}(\omega_1)$ vs p$T_{1P}(\omega_2)$ plots for

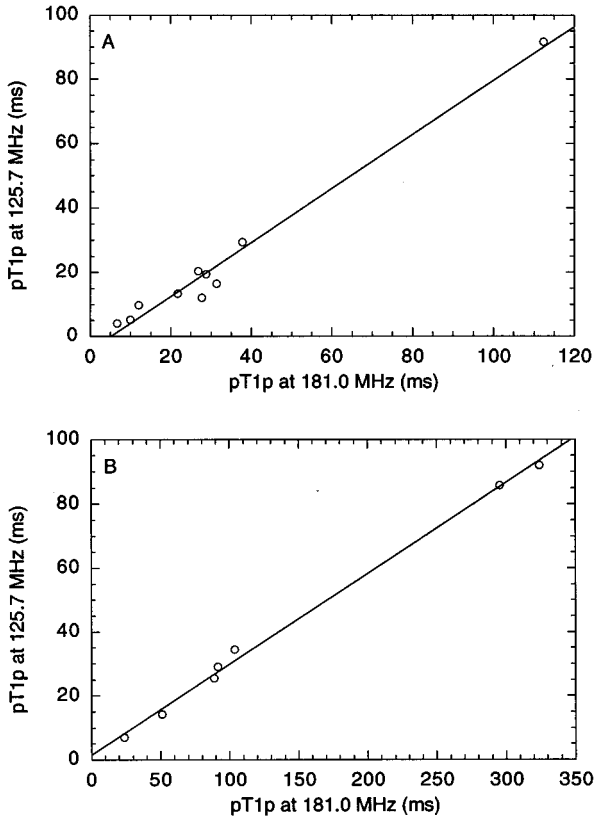

FIGURE 4: Plots of pT_{1P} at 181.0 MHz vs pT_{1P} at 125.7 MHz for (A) AKe·Mn[U-^{13}C]ATP and (B) AKe·[U-^{13}C]AMP·MnGDP complexes.

the ^{13}C nuclei, which are shown above to be independent of the cation−nucleus distances (see Theoretical Details). Examples of linear plots of pT_{1P}(181 MHz) vs pT_{1P} (125.7 MHz) are shown in panels A and B of Figure 4 for AKe·[U-^{13}C]ATP and AKe·[U-^{13}C]AMP·GDP complexes, respectively. Three such linear plots are made for each complex, yielding different values of slopes and intercepts (theoretically, only two of the slopes are independent).

Since pT_{1P} vs ω_I^2 is linear for the AKe·MnATP complex, eqs 11−13 are applicable. A computer fit of the three slopes, $R(\omega_1,\omega_2)$, readily yields the only unknown parameter $\tau_C = 1.4$ ns, and τ_M is similarly evaluated to be 0.5 ms from the intercept data. The rotational correlation time, τ_R, of the AKe complexes was found to be ∼20 ns from the TRNOESY data (*2*). Thus, according to eq 5, a frequency-independent value of $\tau_C = 1.4$ ns yields $\tau_{S1} = 1.5$ ns at the three frequencies, implicitly requiring that $(\omega_S\tau_V)^2 \ll 1$ in this frequency range (see eq 6). The ω_S values corresponding to the three ^{13}C frequencies employed, viz., 75.4, 125.7, and 181 MHz, are 1.24×10^{12}, 2.06×10^{12}, and 2.98×10^{12} s^{-1}, respectively, leading to $\tau_V \leq 10^{-13}$ s to satisfy the condition $(\omega_S\tau_V)^2 \ll 1$. According to eq 8, a value of $\tau_{S1} = 1.5$ ns corresponds to $B\tau_V = 1.37 \times 10^8$ s^{-1}. Therefore, $B \geq 1.37 \times 10^{21}$ s^{-2} in this case.

On the other hand, since pT_{1P} vs ω_I^2 is nonlinear for the AKe·AMP·MnGDP complex, τ_C has a contribution from a frequency-dependent τ_{S1} and the slopes of p$T_{1P}(\omega_1)$ vs p$T_{1P}(\omega_2)$ are given by eq 10. A computer fit of the three sets of slope and intercept values yielded a value of 1.5 ms for τ_M and $\tau_V/B = 2.1 \times 10^{-33}$ s^{-3}. The fact that τ_V/B was constant, although τ_V and B could be varied to obtain a fit,

Table 3: Mn−^{13}C Distances Determined from Relaxation Measurements and Molecular Modeling for AKe·Mn[U-^{13}C]ATP and AKe·[U-^{13}C]AMP·MnGDP Complexes[a]

	AKe·MnATP		AKe·AMP·MnGDP	
spin pair	NMR	model	NMR	model
Mn−C2	11.4	11.0	10.6	10.8
Mn−C4	9.2	9.1	9.5	9.4
Mn−C5	8.1	8.3	8.3	8.3
Mn−C6	9.2	9.0	9.2	8.7
Mn−C8	7.1	7.1	7.1	7.8
Mn−C1′	9.9	9.2	11.2	10.2
Mn−C2′	8.7	8.3	8.7	9.5
Mn−C3′	9.2	8.6	9.5	9.6
Mn−C4′	8.5	9.1	11.2	10.3
Mn−C5′	7.5	7.0	9.3	9.5

[a] The NMR-determined distances were calculated using eqs 3−6 with $C = 512$ Å $s^{-1/3}$ and the following parameters: $\tau_C = 1.4$ ns and $\tau_M = 0.5$ ms for the ATP complex (τ_C is frequency independent); $\tau_C = 6.1$, 3.6, and 1.5 ns for 181, 125.7, and 75.4 MHz, respectively, and $\tau_M = 1.5$ ms for the AMP complex (τ_C is frequency dependent). Distances from the model are mean values of a structural ensemble for the corresponding nucleotide. Errors in distances from molecular modeling are ±0.2 and ±0.5 Å for the NMR measurements.

shows that τ_{S1} is given by eq 9, which applies when $(\omega_S\tau_V)^2 \gg 1$. Thus, with $\tau_V \geq 2.5 \times 10^{-12}$ s to satisfy the condition $(\omega_S\tau_V)^2 \gg 1$ for the ω_S values given above, $B \geq 1.2 \times 10^{21}$ s^{-2}. This value of B is comparable to that for the ATP complex. Substituting $(\tau_V/B) = 2.1 \times 10^{-33}$ s^{-3} into eq 9 gives τ_{S1} values of 1.6, 4.5, and 9.3 ns at ^{13}C frequencies of 75.4, 125.7, and 181 MHz, respectively. With a τ_R of 20 ns, the corresponding τ_C values are 1.5, 3.7, and 6.4 ns, respectively (see eq 5). The contrasting frequency dependence in Figure 3 occurs because the value of τ_V is larger in the AMP complex by a factor of about 25 compared to that in the ATP complex.

The 10 ^{13}C−Mn(II) distances calculated for the two complexes are given in Table 3. Using these distances and other parameters entering the theory in eqs 1−6, the T_{1M} values were back-calculated and are plotted against the corresponding experimental values. These plots are shown in Figure 5 for the data at all three frequencies. The agreement between the points in these plots and a straight line of unit slope suggests that the analysis leading to the determination of one set of $f(\tau_C)$ and τ_M values compatible with all 10 ^{13}C relaxation rates in each complex is appropriate.

Structural Characterization. A starting structure was taken from one of the conformers for ATP and for AMP for which the adenosine conformations have been determined from TRNOESY experiments as reported in the preceding paper (*2*). Mn(II) was added to the starting molecule, with a formal charge of +2 assigned to the cation. Accurate estimates of partial charges for the hydroxyl oxygens of the phosphate groups are not readily available. With a formal charge of −1 assigned to these groups, the Gasteiger−Marsili (*19*, *20*) method returned values ranging between −0.57 and −0.82 for the different nonbridge oxygen atoms in the phosphate chain. The correction appears to take the effect of resonance delocalization into account, and these values were, therefore, used in subsequent modeling simulations. On this structure, MD simulated annealing calculations were performed, in which the nucleotide structure is repeatedly heated to 2000 K and allowed to equilibrate at this temperature for 2 ps,

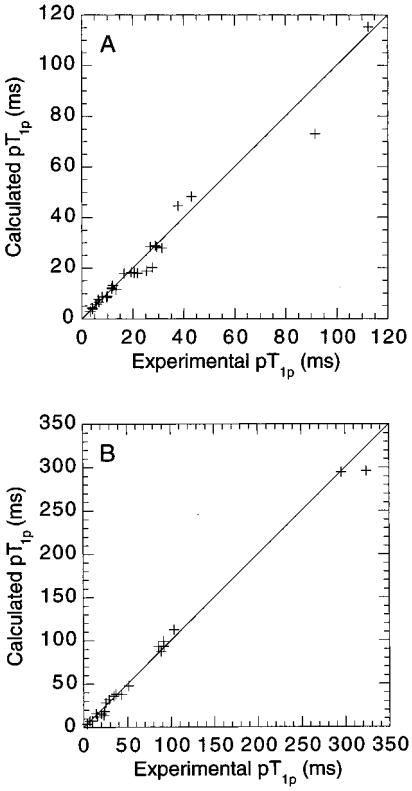

FIGURE 5: Plot of calculated and measured pT_{1P} of ^{13}C for (A) AKe·Mn[U-^{13}C]ATP and (B) AKe·[U-^{13}C]AMP·MnGDP complexes. Parameters used for back-calculations were the *r*-values for each carbon given in Table 3, $C = 512$ Å $s^{-1/3}$, and B and τ_V values given in the legend of Figure 3. The solid line through the origin is drawn with a slope of unity.

followed by exponential cooling to 0 K over 5 ps. Molecular mechanics energy was then minimized on these nucleotide structures with the Mn(II)−^{13}C distances, determined above, as added constraints. At this point, the ambiguity regarding the effect of resonance delocalization on the charge appropriate for the deprotonated hydroxyl oxygens, mentioned above, was reexamined by repeating the simulated annealing and energy minimization, with the Mn(II)−^{13}C distance constraints included, for different methods of charge delocalization assignment available with the SYBYL software package. These simulations yielded identical energy-minimized structures for the different runs, suggesting that the distance constraints overcome variabilities in these force field parameters arising from ambiguities in the charge delocalization assignments.

For ATP, the calculations yielded 14 converged structures. These 14 structures form three groups of 5, 5, and 4 structures of nearly identical geometries. The torsion angles characterizing the adenosine conformations agreed with each other for all three groups. The glycosidic angle, χ, is found to be 51° ± 2°, in agreement with the TRNOESY determined value (*2*). The other torsion angles have changed, however (see Table 4). One structure from each of the three conformations is illustrated in Figure 6A. All three structures are compatible with the Mn−^{13}C as well as the TRNOESY distance constraints. For AMP, 18 structures converged and are shown in Figure 6B. The glycosidic torsion angle, χ, was 45° ± 2° for all 18 structures, whereas the TRNOESY determined value was 37°. All torsion angles are given in Table 4, in which the values from X-ray data are shown for

Table 4: Various Torsion Angles Characterizing the NMR-Determined Enzyme-Bound Nucleotide Structures, Determined by NMR and Molecular Modeling[a]

designation	torsion	[U-^{13}C]ATP (model)	[U-^{13}C]AMP (model)	AMPPNP (X-ray)	AMP (X-ray)
χ	O4′−C1′−N9−C8	50	45	83	−4
γ	O5′−C5′−C4′−C3′	37	37	37	74
ϕ_1	C4′−C5′−O5′−Pα	164	−84	−170	−117
υ_0	C4′−O4′−C1′−C2′	−11	−19	4	−9
υ_1	O4′−C1′−C2′−C3′	9	10	14	−19
υ_2	C1′−C2′−C3′−C4′	−4	2	−26	38
υ_3	C2′−C3′−C4′−O4′	−3	−13	26	−42
υ_4	C3′−C4′−O4′−C1′	9	20	−20	35

[a] The values given are ±2°. The corresponding values in the X-ray data (*24*) are shown for comparison. The definitions for the various torsion angles conform to those by Sanger (*21*).

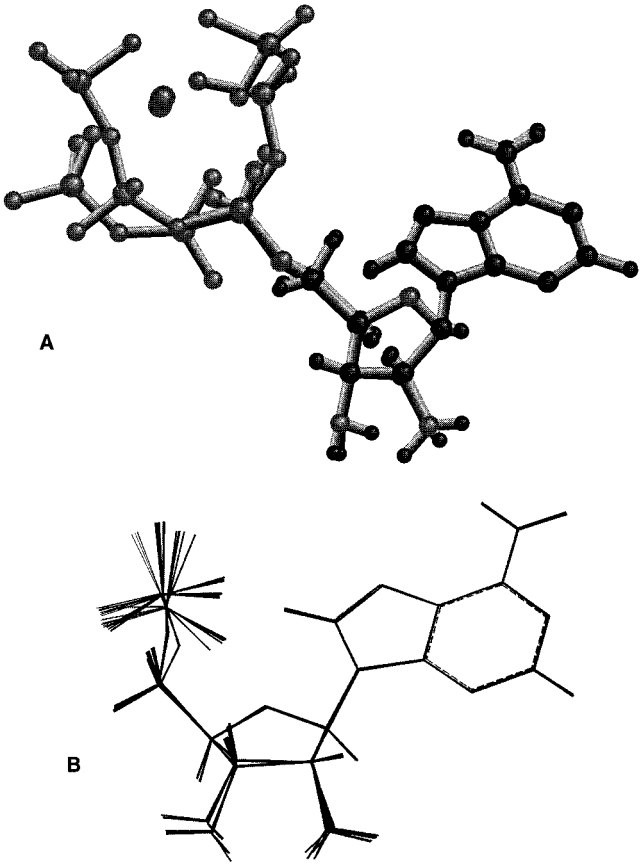

FIGURE 6: Conformations of (A) ATP and (B) AMP in (A) AKe·M(II)ATP and (B) AKe·AMP·M(II)GDP complexes, obtained by applying distance constraints, determined from both TRNOESY and the relaxation measurement in the presence of paramagnetic cations, in molecular modeling. The cation is included in the figure for each nucleotide.

comparison. It is evident that the X-ray and NMR-determined adenosine conformations are significantly different.

DISCUSSION

The distances characterizing the conformation of each enzyme-bound nucleotide determined in this and the preceding paper (*2*) represent virtually a complete set of structural data that may be obtained from liquid-state NMR methodologies. Another set of relaxation enhancement measurements could be made, in principle, with [U-^{15}N]nucleotide in the presence of Mn(II). These distances are relevant to the orientation of the phosphate chain, which is chelated by the cation, with respect to the rigid and planar adenine fragment. Adequate data are available for the determination of this orientation through ^{13}C measurements presented in this paper.

The strategy of stepwise acquisition of distance data, first to locate the cation with respect to the phosphate chain by means of ^{31}P relaxation measurements with Co(II) as the cation, second to determine the glycosidic torsion and sugar pucker in the adenosine fragment through TRNOESY measurements, and third to determine the distances of all 10 ^{13}C nuclei in adenosine from Mn(II) through the enhancement of ^{13}C relaxation rates, was necessary to arrive at a complete characterization of each nucleotide as a whole. This necessity arises due to the fact that free nucleotides are floppy molecules with large amplitude mobilities. The approach was initiated with the premise that the bound nucleotide assumes a single preferred conformation for catalysis, and the results obtained appear to justify this view. There are other assumptions implicit in this strategy. For instance, the three sets of measurements mentioned above have been performed with three different cations in the complexes, Co(II) and Mn(II) for ^{31}P and ^{13}C relaxation measurements, respectively, and Mg(II) for TRNOESY measurements. Mg(II) is the natural activator, and Mn(II) and Co(II) are substituent activators. Therefore, the implicit assumption is that the productive conformations of the enzyme-bound nucleotides with the three cations are close enough that the distance data gathered separately in the three sets of experiments may be pooled together to characterize the conformation of the nucleotide in E·M·S complexes. The fact that the distance data set is implicitly overdetermined and that internal consistency is an essential element in deducing compatible conformations makes the results reliable.

The glycosidic torsion angle, χ, for AMP in the E·AMP·M(II)GDP complex, which was deduced to be 37° ± 5° from the TRNOESY data (*2*), changed to 45° ± 2° when the Mn−^{13}C distances obtained here were introduced as additional constraints. This new value is in good agreement with the range 51° ± 7° determined from TRNOESY measurements on a number of adenine nucleotides bound to ATP-utilizing enzymes (*22*). Thus, the glycosidic torsion angles for both enzyme-bound nucleotides are consistent with the suggestion of a common motif for the recognition and binding of the adenosine moiety of adenine nucleotides binding to ATP-utilizing enzymes (*22*). The availability of computer programs for iterative modeling based on distance constraints imposed on molecular dynamics was critical in order to arrive at the final structures.

The contrasting frequency dependence of ^{13}C relaxation times in the two different nucleotide complexes of the enzyme is analogous to what has been observed in published measurements on ATP and ADP complexes of 3-phosphoglycerate kinase (*4*) and creatine kinase (*16*). In those complexes, the tridentate MnATP complexes show a larger value of B and a longer value of τ_V (by a factor of over 25) compared to the ADP complexes. Thus, the frequency dependence of ^{13}C relaxation times (pT_{1P} vs ω_I^2) was nonlinear for the ATP complexes and was linear for the ADP complexes. In the present work, the B values are similar in AKe·MnATP and AKe·AMP·MnGDP complexes, consistent with the fact that both complexes are bidentate. On the other hand, the τ_V value for the AKe·AMP·MnGDP complex is larger (by a factor of over 25) compared to that in the AKe·MnATP complex, suggesting that the fluctuations in the crystal field occur more rapidly, and consequently the cation may be more accessible to the solvent in the latter. Considering that both nucleotide binding sites are occupied in the AMP complexes, the lower accessibility of the cation to the solvent in this case appears reasonable.

The NMR-determined nucleotide conformations differ from those in published X-ray crystallography. This difference was observed for the adenosine conformations determined from TRNOESY data (*2*). The set of Mn−^{13}C distances determined here could not be compared with the X-ray structures as the cation was not located in the X-ray data (*23*, *24*). Overlays of NMR and X-ray-determined structures of AMP, and of ATP (NMR) overlaid by AMPPNP (X-ray), are shown in panels B and A of Figure 7, respectively. These panels, prepared by approximately superposing the ribose regions of the nucleotides, indicate the extent of divergence between the structures determined by NMR and X-ray crystallography. The X-ray data are derived with ATP analogues, sometimes of necessity, to avoid ATP hydrolysis during crystallization. In addition, location of the cation in the crystal structure was either not possible or not unequivocal, presumably due to interference from anions in the crystallization medium. The crystallization process traps the bound nucleotide in a specific conformation, which may well be fortuitously productive but not guaranteed to be so. The NMR measurements, made in solution phase, on natural substrates, in which the cation is unambiguously placed at the active site, avoid the limitations in the X-ray data and may be the most appropriate ones to be considered for the purpose of identifying the catalytically productive conformations.

It is a generally accepted paradigm of structural biochemistry that a prerequisite for understanding the molecular basis of enzyme catalysis is a knowledge of the structure of the productive conformation of the substrate and its protein environment. The information on the protein environment at the active site of AK, determined from NMR is incomplete and fragmentary (*25*−*28*). It should be noted in this context that the molecular mass of AK is among the lowest of ATP-utilizing enzymes. While considerable protein structural data were acquired for some proteins of this size, the work of Tsai's group on chicken muscle AK being an excellent example (*25*, *28*), the characterization of the binding pocket is far from comprehensive. For heavier proteins the NMR data are nonexistent, whereas X-ray crystallography has been

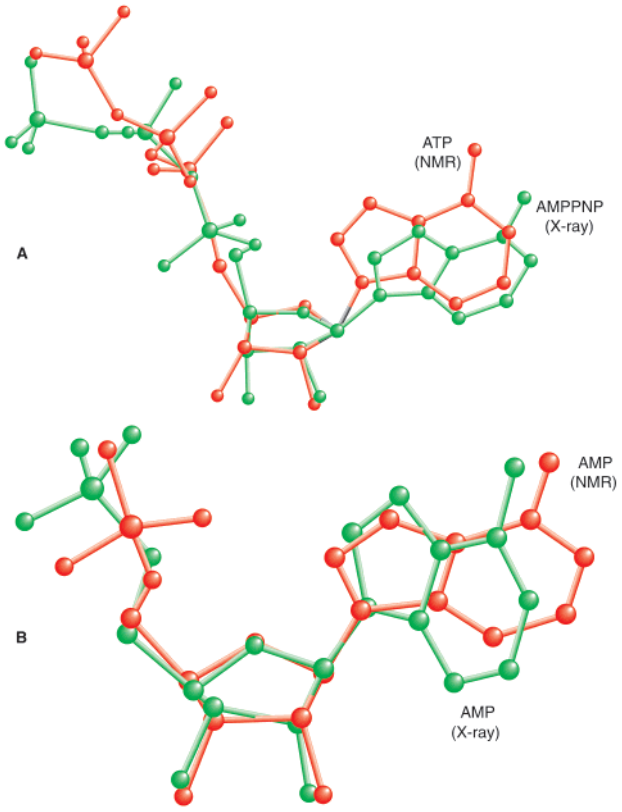

FIGURE 7: Overlay of NMR-determined AKe-bound (A) ATP and (B) AMP structures on AMPPNP and AMP from the crystal structure of AKe·AMP·AMPPNP (*24*), respectively, by superposing on the heavy atoms on the ribose ring. One of the three structures in Figure 6A is shown for ATP. The glycosidic orientations of both ATP and AMP, as well as the phosphate chain orientations, are noticeably different from those of the X-ray results. For clarity, the locations of protons and cations, which are not known in the X-ray structures, are also not shown for the NMR-determined structures in the figure.

prolific in this regard (*23*, *24*, *29*−*34*; also see references cited in the Supporting Information attached to ref 2). Thus, while the substrate conformations determined by crystallographic research may not be as appropriate for catalytic activity as those obtained by NMR, crystallographic data are the best means to acquire structural information on the protein environment at the active site. Crystal structures have been published for the AKe·AMP·AMPPNP complex (*24*) at 2.0 Å resolution and AKe·AP_5A complex (*23*) at 1.9 Å resolution. It is therefore attractive to examine the compatibility of the NMR-determined nucleotide conformations presented here with published X-ray determined enzyme−complex structures by iterative computer methods for docking the structures together. Such studies are currently in progress, and the results obtained will be presented soon.

ACKNOWLEDGMENT

The authors are grateful to Professor Paul Rösch, Universität of Bayreuth, Bayreuth, Germany, and his research group for providing us with the expression system and associated procedures for preparing the protein, to Dr. Nagarajan Murali, National High Magnetic Field Laboratory (NHMFL), Tallahassee, FL, for help and advice with experiments at 720 MHz performed there, and to Dr. Daniel H. Robertson at the Facility for Computational Molecular and Biomolecular Science, IUPUI, for helpful suggestions.

Thanks are due to Drs. Bruce D. Ray, Steve Landy, Gotam Jarori, Vidya Raghunathan, Mei H. Chau, Ms. Xiaoyuan Lu, and Ms. Marina Lyshevski of the NMR group at IUPUI for assistance received in various ways during this research.

REFERENCES

1. Nageswara Rao, B. D., and Ray, B. D. (1992) *J. Am. Chem. Soc. 114*, 1566−1573.
2. Lin, Y., and Nageswara Rao, B. D. (2000) *Biochemistry 39*, 3636−3646.
3. Ray, B. D., Rösch, P., and Nageswara Rao, B. D. (1988) *Biochemistry 27*, 8669−8676.
4. Raghunathan, V., Chau, M. H., Ray, B. D., and Nageswara Rao, B. D. (1999) *Biochemistry 38*, 15597−15605.
5. Reinstein, J., Brune, M., and Wittinghofer, A. (1988) *Biochemistry 27*, 4712−4720.
6. Noda, L. (1973) in *The Enzymes*, Vol. 8, pp 279−305, Academic Press, New York.
7. Brune, M., Schumann, R., and Wittinghofer, A. (1985) *Nucleic Acids Res. 13*, 7139−7151.
8. Reinstein, J., Vetter, I. R., Schlichting, I., Rösch. P., Wittinghofer, A., and Goody, R. S. (1990) *Biochemistry 29*, 7440−7450.
9. Levitt, M. H. (1982) *J. Magn. Reson. 48*, 234−264.
10. James, T. L. (1975) in *NMR in Biochemistry*, pp 177−210, Academic Press, New York.
11. Mildvan, A. S., and Gupta, R. K. (1978) *Methods Enzymol. 49*, 322−359.
12. Villafranca, J. J. (1984) in *Phosphorus-31 NMR: Principles and Applications* (Gorenstein, D. G., Ed.) pp 155−174, Academic Press, New York.
13. Jarori, G. K., Ray, B. D., and Nageswara Rao, B. D. (1985) *Biochemistry 24*, 3487−3494.
14. Ray, B. D., and Nageswara Rao, B. D. (1988) *Biochemistry 27*, 5579−5585.
15. Jarori, G. K., Ray, B. D., and Nageswara Rao, B. D. (1989) *Biochemistry 28*, 9343−9350.
16. Ray, B. D., Chau, M. H., Fife, W. K., Jarori, G. K., and Nageswara Rao, B. D. (1996) *Biochemistry 35*, 7239−7246.
17. Vasavada, K. V., and Nageswara Rao, B. D. (1989) *J. Magn. Reson. 81*, 275−283.
18. Jones, A. J., Winkley, M. W., Grant, D. M., and Robins, R. K. (1970) *Proc. Natl. Acad. Sci. U.S.A. 65*, 27−30.
19. Gasteiger, J., and Marsili, M. (1980) *Tetrahedron 36*, 3219−3228.
20. Marsili, M., and Gasteiger, J. (1980) *Croat. Chem. Acta 53*, 601−614.
21. Sanger, W. (1984) in *Principles of Nucleic Acid Structure* (Cantor, C. R., Ed.) pp 9−28, Springer-Verlag, New York.
22. Murali, N., Lin, Y., Mechulam, Y., Plateau, P., and Nageswara Rao, B. D. (1997) *Biophys. J. 70*, 2275−2284.
23. Müller, C. W. and Schulz, G. E. (1992) *J. Mol. Biol. 224*, 159−177.
24. Berry, M. B., Meador, B., Bilderback, T., Liang, P., Glaser, M. and Philips, G. N., Jr. (1994) *Proteins: Struct., Funct., Genet. 19*, 183−198.
25. Tsai, M.-D., and Yan, H. (1991) *Biochemistry 30*, 6806−6818.
26. Vetter, I. R., Reinstein, J., and Rösch, P. (1990) *Biochemistry 29*, 7459−7467.
27. Vetter, I. R., Konrad, M., and Rösch, P. (1991) *Biochemistry 30*, 4137−4142.
28. Yan, H., and Tsai, M.-D. (1991) *Biochemistry 30*, 5539−5546.
29. Müller, C. W., Schlauderer, G. J. Reinstein, J., and Schulz, G. E. (1996) *Structure 4*, 147−156.
30. Egner, U., Tomasselli, A. G., and Schulz, G. E. (1987) *J. Mol. Biol. 195*, 649−658.
31. Müller, C. W., and Schulz, G. E. (1988) *J. Mol. Biol. 202*, 909−912.
32. Schulz, G. E., Müller, C. W., and Diederichs, K. (1990) *J. Mol. Biol. 213*, 627−630.
33. Schlarder, G. J., and Schulz, G. E. (1996) *J. Mol. Biol. 256*, 223−227.
34. Abele, U., and Schulz, G. E. (1995) *Protein Sci. 4*, 1262−1271.

BI992460E